JOURNAL OF MATERIALS SCIENCE 25 (1990) 619–623

High pressure synthesis and electrical properties of $BaTiO_{3-x}F_x$

TADASHI ENDO, TETSURO KOBAYASHI, TSUGIO SATO, MASAHIKO SHIMADA
Department of Molecular Chemistry and Engineering, Faculty of Engineering, Tohoku University, Aoba, Sendai 980, Japan

The substitution of fluorine for oxygen in $BaTiO_3$ was investigated by the reaction of BaO_2, BaF_2, TiO_2 and Ti under the conditions of 3.0 GPa and 1300° C for 2 h. $BaTiO_{3-x}F_x$ solid solutions were obtained as a single phase in the region of $0 \leqslant x \leqslant 0.1$. The X-ray diffraction data showed that the symmetrical change from tetragonal to cubic form occurred at $x = 0.08$ at room temperature. Also, the solid solutions were characterized by TG-DTA analysis, ESCA spectroscopy and diffusion reflectance spectroscopy. As a result, the existence of Ti^{3+} was verified. The electrical resistivities of $BaTiO_{3-x}F_x$ were in the range from $4\,\Omega$ cm for $x = 0.05$ to $30\,\Omega$ cm for $x = 0.1$ at 300 K and the relationship between ln ϱ and $1\,000\,T^{-1}$ was linear. The thermoelectric powers at 300 K were $-250\,\mu V\,K^{-1}$ for $x = 0.05$ and $-130\,\mu V\,K^{-1}$ for $x = 0.1$. The electrical property of the solid solution was discussed on the basis of a conventional band model which involved localized donor levels associated with oxygen vacancies.

1. Introduction

$BaTiO_3$ is well known as a ferroelectric material with the Curie temperature of 120° C [1]. At the Curie temperature, the perovskite unit cell undergoes tetragonal-cubic phase transformation, accompanied by a sharp change in dielectric constant. The dielectric constant maximum is often used for materials with very high capacitance. Pure $BaTiO_3$ ceramics are not always qualified for dielectric use, and are in particular required to improve the temperature characteristics.

Much work has been devoted to non-stoichiometric $BaTiO_3$, both in the structural aspects related to the nature of defects, and in the subsequent electrical properties [2]. In addition, $BaTiO_3$ based dielectrics have positively been modified by some cation substitutions, like Zr for Ti [3], or Sr for Ba [4], and of which Curie temperature could be settled in the vicinity of room temperature. However, their data clearly supported that no change in the valency state of Ti^{4+} ion was occurred. Previous works for the cation substituted system of $(Ba_{1-x}La_x)TiO_3$ have yielded the results which the change from Ti^{4+} to Ti^{3+} would be partially brought by the substitution of La^{3+} for Ba^{2+} ions, which would result in the drastic change of the electrical properties [5]. In contrast, Shirasaki *et al.* [6] reported that when the substitution of La^{3+} for Ba^{2+} was introduced the formation of cation deficiencies in both 12-coordination and 6-coordination sites in the perovskite structure, and no valency change for Ti^{4+} sites was found.

On the other hand, little information would be obtained for both concerning the effect of anion replacements on the crystal structure and the electrical properties in the anion substituted $BaTiO_3$ based ceramics. In the system $BaTiO_{3-x}F_x$, Sych *et al.* [7] have carried out the synthesis of $BaTiO_{2.95}F_{0.05}$ using the coprecipitation method. Bradley [8] reported that the solid solution of $PbTiO_{3-x}F_x$ was not obtained as the perovskite-type structure, but as the pyrochlore-type structure in $Pb_2Ti_2O_5F_2$. Rüdorff *et al.* [9] also reported the synthesis of the perovskite-type oxyfluorides such as $LiNbO_2F$, $RbNbO_2F$ and $KNbO_2F$. We have hitherto undertaken the study of the anion substituted system with the rutile structure and the perovskite structure, in which the first row transition elements changed their apparent valency states depending on the x value in $MO_{2-x}F_x$ and $BaMO_{3-x}F_x$ (M = the first row transition elements), and the results of preparation and electrical properties in $TiO_{2-x}F_x$ with rutile structure were reported [10].

In this paper, the synthesis and the characterization of the perovskite type solid solutions of $BaTiO_{3-x}F_x$ are described. The results reveal the existence of Ti^{3+} ions in the present solid solution which have not been found before in the cation substituted solid solution with perovskite structure. Our results also lead us to understand some effects of the replacement of O ions by F ions on the electrical properties.

2. Experimental procedure

Analytical grade BaO_2, BaF_2, TiO_2 (anatase) and Ti powders were used as starting materials. Mixtures were prepared in the desired proportions according to the equation of $(1 - x/2)BaO_2 + x/2\ BaF_2 + 1/2\ TiO_2 + 1/2\ Ti \rightarrow BaTiO_{3-x}F_x$, and then formed into a paste by mixing intimately with ethanol for 1–2 days in an agate mortar within a N_2 filled dry box.

In order to prevent the oxidation of the reactant during the high pressure experiments, the resulting

0022-2461/90 $03.00 + .12 © *1990 Chapman and Hall Ltd.*

mixture was pelletized under the pressure of 100 MPa at room temperature and then sealed in a cylindrical platinum capsule. The identical capsule was arranged in the high pressure cell assembly, which consisted of a NaCl sleeve as the pressure medium and a carbon tube as the heater. Reaction conditions within the high pressure apparatus were 3.0 GPa and 1300° C for 2 h. The detailed information on the high pressure experiments were described elsewhere [10]. The sample was quenched within a few minutes to room temperature prior to the release of applied pressure.

The phases of samples were identified by means of a Rigaku X-ray powder diffractometer system (the Ni-filtered CuKα radiation). The integrated intensity and the position of reflections were measured at the scanning rate of 0.25° min^{-1}. Silicon powders were used as an internal standard. Accurate unit cell parameters of solid solutions were determined using a least-square refinement.

The chemical compositions of solid solutions were precisely determined after dissolving the sample into hot conc. HNO_3. The contents of Ti and Ba were measured by use of a Seiko Denshi Ind. SPS 1200 ICP emission spectrometer. Also, the contents of Ti and F were determined by a colorimetric analysis reported in Ref. [10].

Simultaneous thermogravimetry (TG) and differential thermal analysis (DTA) were carried out with a Rigaku Denki Thermoflex high-temperature apparatus at a heating rate of 10° C min^{-1} in air. Al_2O_3 was used as a reference material. The fracture surface of the sample was observed under a JEOL JSM-T20 scanning electron microscope (SEM). The binding energies of Ba, Ti, O and F were measured at room temperature by using an Electron spectrometer for chemical analysis (Shimazu ESCA-750). The samples were directly inserted into the spectrometer and the ESCA data were acquired at about 10^{-9} Torr. The peak positions of each element were relatively corrected by using that of C_{1s} (285.0 eV).

The d.c. electrical resistance was measured by means of a standard four-probe method in the temperature range of 80–300 K. Thermoelectromotive forces were measured using two d.c. digital multimeters or a multilogging meter by applying a temperature gradient along the length of a sample ranging from 3 to 5° C in the temperature range of 80–300 K. Copper metal was used as an electrode. The values of thermoelectric power were estimated from the slopes of temperature difference versus thermoelectromotive force.

3. Experimental results and discussion

According to the chemical analysis and the X-ray powder diffraction data, the solid solutions of $BaTiO_{3-x}F_x$ ($0 \leqslant x \leqslant 0.1$) could be prepared as single phases, which were completely identified as a perovskite-type structure. Figure 1 shows the relationship between lattice parameters and x values. When the x values increased within the solid solution, the a axis increased, whereas the c axis decreased linearly. Then, the crystal symmetry was changed from tetragonal to cubic form at $x = 0.08$. The cell constant of cubic form slightly decreased with increasing x values. The structure can be regarded as a cubic close-packed lattice in which the Ti atoms are located at the corners, the O atoms at the centres of the twelve cube edges and the Ba atoms at the centre of the cubic. Since the change of cell constant was directly reflected to that of the bonding distance between Ti and anion, the observed shrinkage would be due to the difference in ionic radii between O^{2-} (0.14 nm) and F^- (0.133 nm) [11]. Also, the replacement of F^- for O^{2-} positively contributed to the structural stability of the cubic phase. However, it was not still understood why the symmetrical change within the perovskite structure occurred at $x = 0.08$ of $BaTiO_{3-x}F_x$.

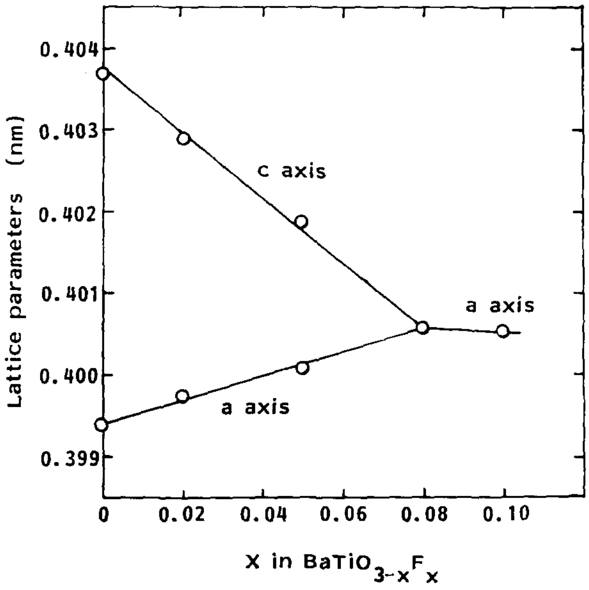

Figure 1 The lattice parameters dependence of x in $BaTiO_{3-x}F_x$.

Figure 2 shows the SEM photograph of the fracture surface of cubic $BaTiO_{2.92}F_{0.08}$ in sintered body. In this photograph, some elongated grains of 1–10 μm were distributed at random. The observed morphology suggested that the individual grains crystallized in virtue of either the evaporation–condensation of some gas phase or the dissolution–precipitation of some liquid phase in the closed reaction system under high pressure-temperature conditions.

All the solid solutions of $BaTiO_{3-x}F_x$ had pale blue

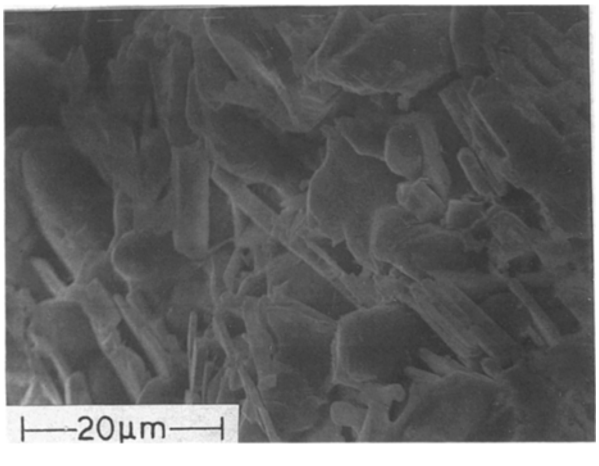

Figure 2 The SEM photograph of the fracture surface of $BaTiO_{2.92}F_{0.08}$.

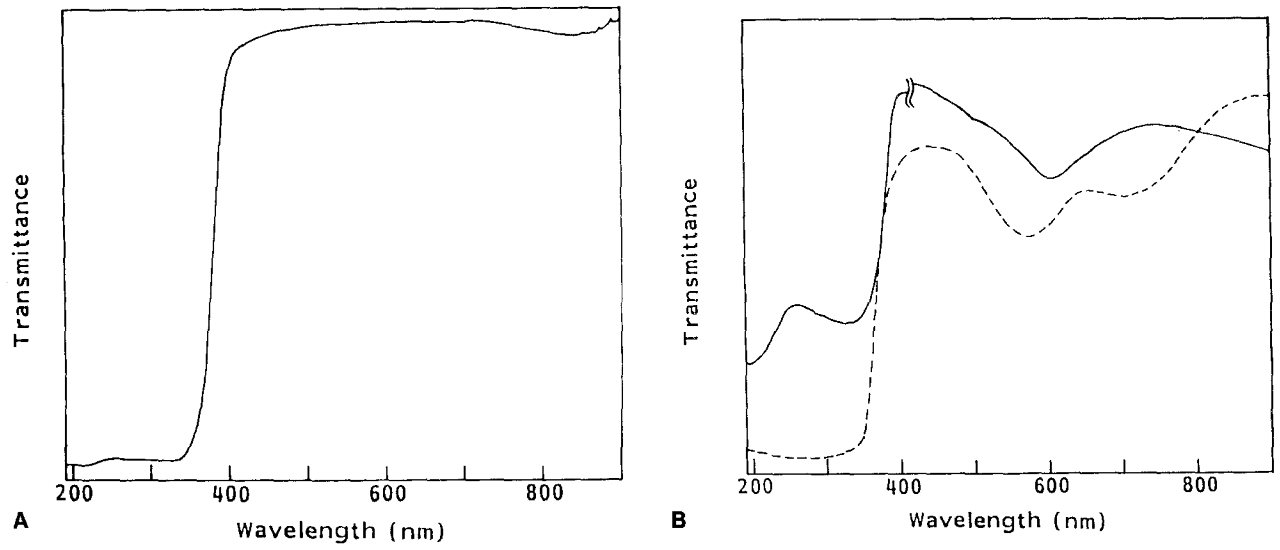

Figure 3 The reflection spectra of tetragonal BaTiO$_3$ (A), and cubic BaTiO$_{2.9}$F$_{0.1}$ (——) and TiF$_3$ (- - -) (B).

colour. Figure 3 shows the reflection spectra of tetragonal BaTiO$_3$ (A) and cubic BaTiO$_{2.9}$F$_{0.1}$ (B) at room temperature. Also, the reflection spectrum of TiF$_3$ is illustrated as a broken line in Fig. 3(B).

In spite of difference in the crystal symmetry, the fundamental absorption edge of cubic BaTiO$_{2.9}$F$_{0.1}$ was estimated to be at about 360 nm, which was very similar to that observed for BaTiO$_3$. It is generally agreed that this absorption edge is due to the electron transitions between predominantly the empty, Ti–O antibonding states and the filled, Ti–O bonding states with little admixture of Ba ion wave function. However, the profile in the reflection spectrum of cubic BaTiO$_{2.9}$F$_{0.1}$ was slightly different from that of tetragonal BaTiO$_3$. According to the results reported by Cardona [12], the observed splitting below 360 nm might be elucidated by the effects of the crystal field. On the other hand, a distinctive peak at about 575 nm was identified as the $^2\mathrm{E}_{2g} \rightarrow {}^2\mathrm{T}_g$ transition of Ti^{3+}, because the reflection spectrum of TiF$_3$ also revealed an intense peak at about 570 nm. This result indicated that the solid solutions of BaTiO$_{3-x}$F$_x$ involved the Ti^{3+}–F bondings statistically distributed in the cubic structure. According to the chemical analysis data, the solid solutions contained little oxygen vacancies within experimental errors of 0.01%. Therefore, the general formulation of the solid solutions is written as $\mathrm{BaTi}^{4+}_{1-x}\mathrm{Ti}^{3+}_{x}\mathrm{O}^{2-}_{3-x}\mathrm{F}^{-}_{x}$, assuming the electrical neutrality.

Figure 4 shows the TG–DTA curve of cubic BaTiO$_{2.92}$F$_{0.08}$. The solid solution exothermically decomposed near 600° C in air. Simultaneously, the weight loss of about 0.1% was observed. This value was nearly coincident with the calculated value according to the reoxidation from BaTiO$_{2.92}$F$_{0.08}$ to BaTiO$_3$. An endothermic peak and a drastic weight loss were observed at about 720° C and 850° C, respectively. It was still questionable that a thermal change was encountered at these different temperatures. However, it was clear that such changes were substantially related to the formation of oxygen vacancies in BaTiO$_3$. At 1030° C, the weight loss progressed stepwise. From the X-ray diffraction data, the recovered sample after DTA measurement was identified as tetragonal BaTiO$_3$. In the DTA curve of tetragonal BaTiO$_{2.95}$F$_{0.05}$, no discontinuous change at 1030° C was observed. This thermal change could be regarded to the symmetrical change from cubic to tetragonal phase.

The ESCA spectra were measured in order to clarify the local field of Ba, Ti, O and F. The ESCA spectrum

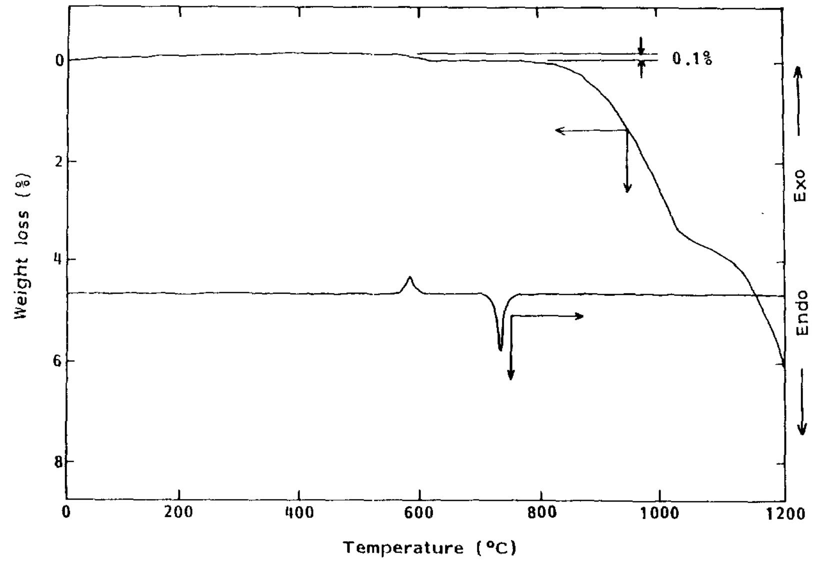

Figure 4 The TG–DTA curve of BaTiO$_{2.92}$F$_{0.08}$ measured in air (heating rate: 10° C min^{-1}).

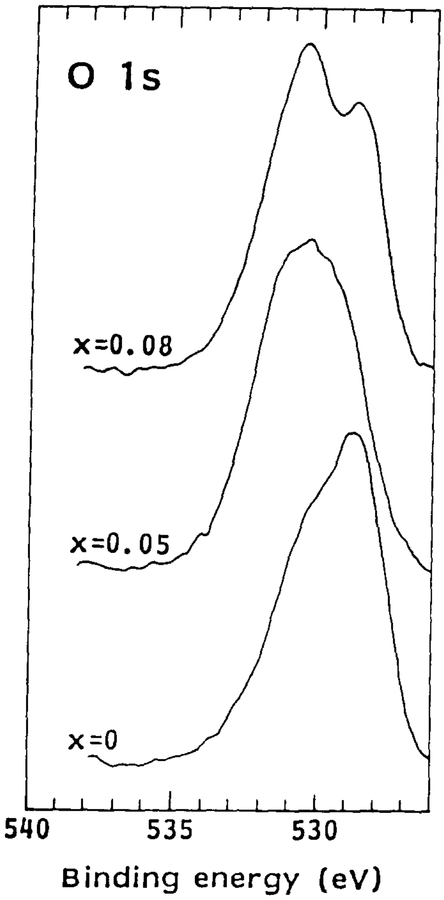

Figure 5 ESCA spectra of O_{1s} for the series of $BaTiO_{3-x}F_x$.

of F_{1s} was relatively weak in intensity, so that the profile failed to be analyzed. The spectra concerning to Ba_{3d} and Ti_{2p} were asymmetrical and broad, and did not show any significant splittings, due to the change of valency state in both tetragonal and cubic phases. On the other hand, the O_{1s} spectra were apparently separated by two or more signals at the interval of a few eV. Figure 5 shows the ESCA spectra of O_{1s} in the cubic ($x = 0.08$) and tetragonal ($x = 0.05$) $BaTiO_{3-x}F_x$, and tetragonal $BaTiO_3$ which was prepared at 1100° C in air, respectively.

The ESCA spectra of O_{1s} consisted of the superimposed signal due to the different binding states of oxygen. With the partial substitution of F^- for O^{2-}, the higher binding energy signal relatively increased in intensity. The present tetragonal $BaTiO_3$ sample contained a small amount of oxygen vacancies, because the present reaction temperature condition above 1000° C in air was considered to form a reduction circumstance [12]. In addition, these defects, in particular surface defects would be expected to influence the efficiency of adsorbed oxygen. In fact, a peak corresponding to the low binding energy side of the O_{1s} signal at 529 eV could be contributed to the existence of adsorbed oxygen as indicated by Pertosa and Michel-Calendini [13].

On the other hand, Devries [14] reported that the structural stability of cubic $BaTiO_3$ was preserved, even at room temperature, by the high concentration of oxygen vacancies. At low concentration of F, the present solid solutions probably contained a small amount of oxygen vacancies. The change in intensity of a peak near 529 eV indicated that some deficiencies, which function as active absorption sites for oxygen, gradually diminished with increasing F^- contents.

Figure 6 shows an Arrhenius plot of logarithm resistivity versus reciprocal temperature for $BaTiO_{3-x}F_x$. Figure 7 shows the temperature dependence of thermoelectric power for $BaTiO_{3-x}F_x$.

Since the thermoelectric power coefficient was negative, the conduction could be characterized by an electron carrier mechanism. With increasing the F^- contents, the thermoelectric power became smaller. As described before, the octahedral distortion around Ti^{4+} sites tended to reduce owing to the subsequent substitution of F^- for O^{2-}. Consequently, the effect of phonon scattering on the electron mobility is considered to substantially disappear.

The linear relationships between $\ln \varrho$ vs $1000\,T^{-1}$ were experimentally found in all solid solutions. This implied that the hopping mechanism proposed by Hurd [15] was not available for elucidating the present results. If the present conduction mechanism was explained by application of a conventional band model, the thermally excited electrons to the π^* conduction band may incidentally be responsible for the conductivities of the present solid solution. The slopes corresponded to the values of activation energy in the range 0.07 to 0.04 eV. However, the resulting values were fairly small, and were not equal to the energy gap between the nonbonding level of Ti^{3+} and the conduction π^* band. As seen in Fig. 6, the two activation

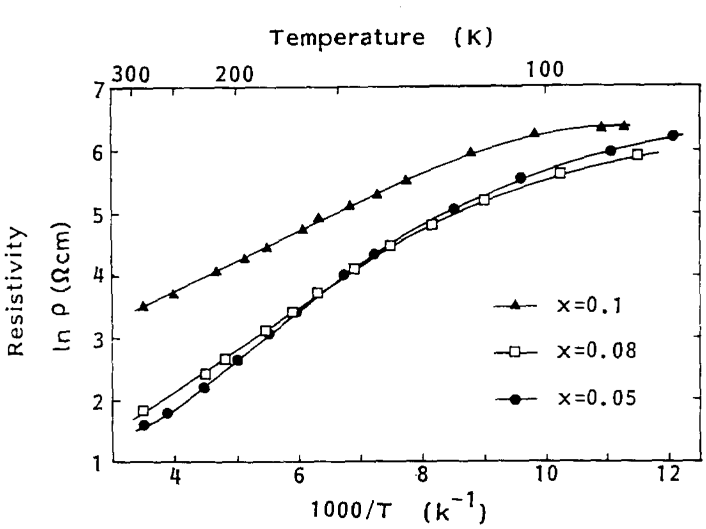

Figure 6 Temperature dependence of electrical resistivity of $BaTiO_{3-x}F_x$.

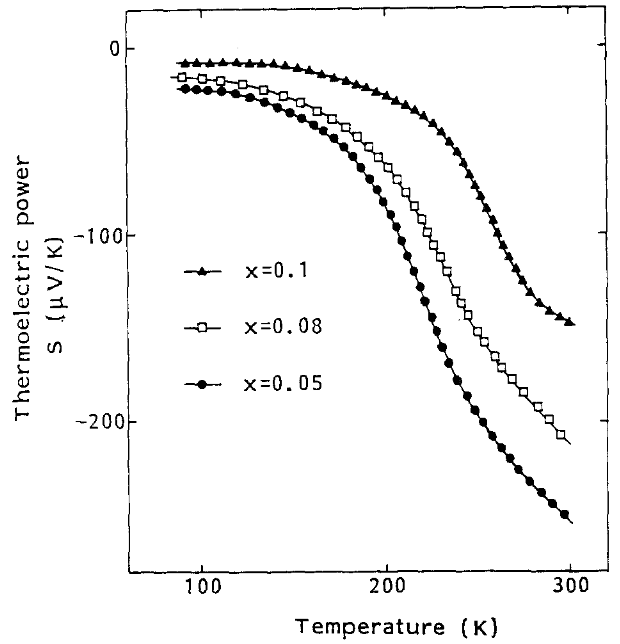

Figure 7 Temperature dependence of thermoelectric power of $\mathrm{BaTiO}_{3-x}\mathrm{F}_x$.

energies of each sample were expected for donor sites, assuming electrons associated with oxygen vacancies. Because of a sufficiently small quantity of donors, the donor electrons would occupy the localized levels without the formation of a donor band [16]. In fact, donor levels lying beneath the bottom of the conduction band could be considered to readily change their positions by virtue of the structural symmetry. When the scattering is assumed to be predominantly governed by the phonon vibrations, the effective electron mobilities in the conduction band would increase with increasing the F^-. In the present solid solution, however, the concentration of oxygen vacancies decreased with increasing the F^- contents. As a result, the increase of the electrical resistivity would be fully elucidated by assumption of which the population of electrons as carrier in donor levels decreased.

4. Conclusions

1. The solid solution of $\mathrm{BaTiO}_{3-x}\mathrm{F}_x$ $(0 \leqslant x \leqslant 0.1)$ could be prepared as a single phase by the reaction of BaO_2, BaF_2, TiO_2 and Ti under the condition of 3.0 GPa and 1300° C for 2 h.

2. Phase change from tetragonal to cubic in perovskite structure was occurred at $x = 0.08$ of $\mathrm{BaTiO}_{3-x}\mathrm{F}_x$.

3. It could be verified that the substitution of F^- for O^{2-} was introduced to the existence of Ti^{3+} ion in $\mathrm{BaTiO}_{3-x}\mathrm{F}_x$.

4. The elemental resistivities of the solid solutions were in the range of 4 Ω cm to 30 Ω cm at 300 K. The thermoelectrical power data indicated that the solid solutions had *n*-type semiconducting characteristics.

5. The conduction mechanism could be explained by application of a band model having the localized donor levels.

Acknowledgements

This work was partly supported by a Grant-in-Aid for Scientific Research on Priority Area from the Ministry of Education, Science and Culture, Japan.

References

1. B. M. WUL and L. F. VERESHCHAGIN, *Comptem. Rend. Acad. Sci. U.S.S.R.* **48** (1945) 634.
2. S. H. WEMPLE, M. DIDOMENNICO and A. JAYARAMAN, *Phys. Rev.* **180** (1969) 547.
3. D. HENNINGS, A. SCHNELL and G. SIMON, *J. Am. Chem. Soc.* **65** (1982) 539.
4. E. ANDRICH, *Electronic Application* **26** (1965) 26.
5. O. SABURI, *J. Phys. Soc. Jpn* **14** (1959) 1159.
6. S. SHIRASAKI, H. HANEDA, K. ARAI and M. FUJIMOTO, *J. Mater. Sci.* **22** (1987) 4493.
7. A. M. SYCH, D. I. BILYK and L. F. BARCHUK, *Inorg. Mater.* **8** (1972) 1130.
8. F. BRADLEY, *J. Amer. Ceram. Soc.* **52** (1969) 114.
9. W. RÜDORFF and D. KRUG, *Z. Anorg. Allg. Chem.* **329** (1964) 211.
10. T. ENDO, N. MORITA, T. SATO and M. SHIMADA, *J. Mater. Res.* **3** (1988) 392.
11. L. H. AHRENS, *Geochim. Cosmochim. Acta* **2** (1952) 155.
12. M. CARDONA, *Phys. Rev.* **140** (1965) A651.
13. P. PERTOSA and F. M. MICHEL-CALENDINI, *Phys. Rev.* **B17** (1978) 2011.
14. R. C. DEVRIES, *J. Amer. Ceram. Soc.* **43** (1960) 226.
15. C. M. HURD, *Phil. Mag.* **50B** (1984) L29.
16. J. B. GOODENOUGH and J. M. LONGO, Landolt–Bornstein, Group III/Vol. 4a Springer-Verlag, New York, Berlin (1970).

Received 17 October 1988
and accepted 13 April 1989